ELSEVIER

Polymer 43 (2002) 4159–4166

polymer

www.elsevier.com/locate/polymer

The effect of molecular weight on the lamellar structure, thermal and mechanical properties of poly(hydroxybutyrate-*co*-hydroxyvalerates)

S. Luo[a,1], D.T. Grubb[a,b,*], A.N. Netravali[a]

[a]*Fiber Science Program, Cornell University, Ithaca, NY 14853, USA*
[b]*Materials Science & Engineering, Cornell University, Ithaca, NY 14853, USA*

Received 12 December 2001; received in revised form 25 March 2002; accepted 27 March 2002

Abstract

A poly(hydroxybutyrate-*co*-hydroxyvalerate) with 9% hydroxyvalerate content has been thermally degraded to give a set of materials of different molecular weights. The effect of molecular weight on the lamellar structure, thermal and mechanical properties was investigated. The long period, lamellar and amorphous thickness all increase as molecular weight increases; their values vary linearly with 1/(molecular weight). Observed melting temperatures increase with molecular weight, following the same functional form, while melting enthalpy and non-isothermal crystallization temperature decrease. Young's modulus varies by 13% with molecular weight; changes in crystallinity cannot explain this effect in detail. Ultimate tensile strength increases rapidly with molecular weight and then levels off at 28.5 MPa above 10^5 g/mol. This can also be seen as a linear variation with 1/(molecular weight). The strain at the point of ultimate tensile strength also increases rapidly up to 10^5 g/mol but then continues to increase at a slower rate.

Keywords: Poly(hydroxybutyrate-*co*-hydroxyvalerate); Structure; Mechanical properties

1. Introduction

In the past few years, biodegradable polymers have attracted much attention as a possible solution to the problems of plastic waste. Poly(hydroxyalkanoates) (PHAs) represent a family of biodegradable polymers synthesized by microorganisms under conditions of nutrient limitation [1,2]. Poly(hydroxybutyrate) (PHB) is the main member of this family. The most serious drawback of PHB is its increasing brittleness with time [3,4]. When the fermentation conditions are carefully controlled, and the bacteria are grown with combinations of substrates, a variety of PHA copolymers are produced. These copolymers have much better physical and mechanical properties than PHB homopolymer [5].

Poly(hydroxybutyrate-*co*-hydroxyvalerates) (PHBVs) are the most important PHA copolymers. They have physical and mechanical properties comparable to conventional thermoplastics such as polyethylene and polypropylene [6,7]. A new type of totally biodegradable and environment-friendly 'Green' composite has been made by combining natural cellulosic fibers with PHBV [8,9]. Such composites could be used in many non-critical applications, such as automobile parts and computer parts, and they can be easily composted after their life times [8,9].

PHB and its copolymers, like other polyesters, are thermally unstable above their melting temperatures [10,11]. Thermal degradation of these polymers occurs by a non-radical, random chain scission mechanism involving a β-CH hydrogen transfer process [10,12]. Grassie et al. [12–14] have extensively studied the principal features, products, and reaction mechanisms of PHB thermal degradation. Addition of conventional stabilizers and antioxidants has been found to have no effect on the thermal stability of PHB and its copolymers [15]. In this paper, PHBVs with different molecular weights were prepared through controlled thermal degradation.

Molecular weight is one of the most important factors governing the properties for a polymer. However, the effect of molecular weight on polymer structure and properties is a very complicated issue, and there are few generally applicable theoretical predictions [16–18]. Even though PHB and its copolymers, especially PHBVs, have attracted a wide interest in the last decade, there has been no complete report on the effect of molecular weight on their structure and properties. In this paper, we describe the effect of molecular

* Corresponding author. Address: Materials Science & Engineering, Cornell University, Ithaca, NY 14853, USA. Tel.: +1-607-255-3683; fax: +1-607-255-2365.

E-mail address: dtg1@cornell.edu (D.T. Grubb).

[1] Present address: Albany International, 156 S. Main Street, Homer, NY 13077, USA.

0032-3861/02/$ - see front matter
PII: S0032-3861(02)00242-2

Table 1
Intrinsic viscosity and $\bar{M}_w$ of PHBVs obtained through thermal degradation

	Time (min)								
	0	1	2	5	10	20	30	40	60
$[\eta]$ (dl/g)	2.13	1.98	1.69	1.36	1.18	0.77	0.64	0.57	0.43
$\bar{M}_w$ (kg/mol)	287	262	213	160	134	77	61	53	37

weight on the lamellar structure, thermal and mechanical properties of PHBVs.

2. Experimental

2.1. Materials

PHBV without plasticizers was provided by the BIOPOL business unit of Monsanto in the form of chips. One-mm thick PHBV films were formed using a Carver Hot Press at 180 °C under 140 MPa pressure. PHBVs with different molecular weights were obtained by varying the thermal processing times under these processing conditions. These PHBVs all have the same chemical composition with 9% hydroxyvalerate (HV) content [19]. Intrinsic viscosity was measured using a Ubbelohde type capillary viscometer. Weight-average molecular weight, $\bar{M}_w$, was calculated using the following equation [20]

$$[\eta] = 1.18 \times 10^{-4} \bar{M}_w^{0.78} \quad (1)$$

where $[\eta]$ is the intrinsic viscosity. Data are presented in Table 1. The films were removed from the hot press and quenched into dry ice and acetone. This mixture is at a temperature much lower than the glass transition temperatures of PHBVs. The quenched films were stored at −5 °C for long-term stability then annealed at 80 °C for 24 h immediately before characterizing their properties.

2.2. SAXS measurements

Small-angle X-ray scattering (SAXS) measurements were made on the F1 beam-line of the Cornell high-energy synchrotron source (CHESS). The F1 station provides a high-brightness beam converging to a focus. The convergence angles are 1 mrad in the horizontal plane and 0.3 mrad in the vertical plane, and the peak intensity was $\sim 5 \times 10^{12}$ photons/(s mm^2).[2] The source is tunable, and in these experiments, 13.63 keV photons (wavelength $\lambda = 0.091$ nm) were used with a collimator of diameter 0.1 mm. Exposure times were 60 s with a sample to detector distance of 750 mm. To reduce air scatter, a chamber filled with helium replaced all but a few centimeters of the air path. The chamber had a beryllium front window and a thin Mylar rear window. The beam stop was kept in contact with the rear window to reduce the effect of wide-angle scattering from the window material. The detector was a 1024 × 1024 CCD with a 50 mm × 50 mm sensitive area.

[2] For more details, see http://www.chess.cornell.edu/Facility/Stations_n_Facilities/CHESS_East/F1_station.htm

2.3. DSC measurements

Thermal analysis was performed using a SEIKO oscillating differential scanning calorimeter, DSC 220C. After calibration with indium, specimens were scanned from −40 to 180 °C at a heating rate of 10 °C/min for the first run. After being held at 180 °C for 2 min, the specimens were cooled down to −40 °C at a cooling rate of 10 °C/min. They were then reheated to 180 °C at the same heating rate of 10 °C/min for the second melting run. Glass transition temperatures were obtained from the first run. Melting temperature, T_m, was taken as the onset of the first melting peak in both first and second runs. The melting enthalpy, ΔH_m, was also measured on both runs. A non-isothermal crystallization temperature, T_c, was obtained from the cooling run.

2.4. Mechanical testing

Strips with dimensions of 90 mm × 10 mm × 1 mm were cut from the annealed PHBV films. Wooden tabs were glued at both ends of the strips to avoid jaw breaks, leaving a gauge length of 50 mm. Tensile tests were performed using an Instron Model 1122 tensile testing machine according to ASTM D 3039-92 at a strain rate of 0.04 min^{-1}. Average values of ultimate tensile strength and its corresponding strain, and Young's modulus were calculated from the stress–strain plots of at least five specimens.

3. Results and discussions

3.1. SAXS analysis

The basic microstructure of the polymer is a stack of alternating thin crystalline lamellae and thin amorphous layers. The average thickness of the repeating structure is called the long period. The size and form of these structures depend strongly on both molecular structure (molecular weight, degree of branching, length and distribution of side chains) and thermal history (cooling rate and crystallization temperature, etc.) [21–23]. SAXS is a very powerful tool for probing the detailed microstructure of semicrystalline polymers. Quantitative analysis of the

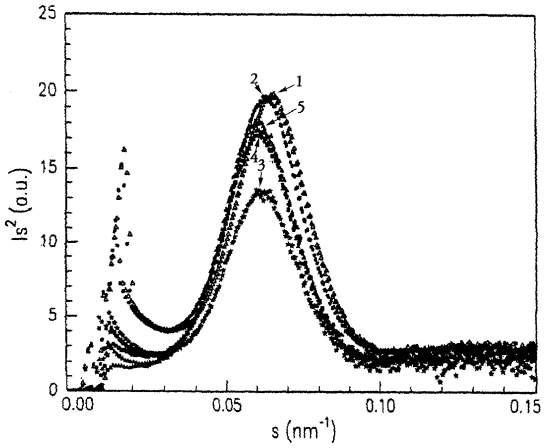

Fig. 1. Profiles of Lorentz-corrected SAXS intensity for PHBVs with different molecular weights. (1) 53 000, (2) 77 000, (3) 134 000, (4) 160 000, (5) 62 000 g/mol.

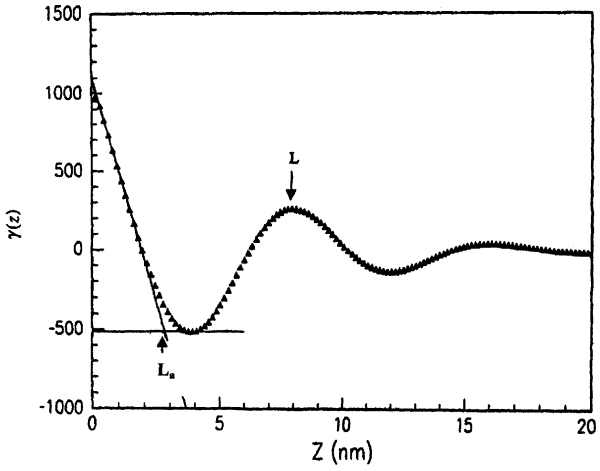

Fig. 2. A typical one-dimensional correlation function for PHBV indicating L = long period, and L_c = lamellar thickness.

SAXS patterns gives the long period (L), the lamellar thickness (L_c), and amorphous layer thickness (L_a).

Fig. 1 shows the Lorentz-corrected SAXS intensity of PHBVs with different molecular weights. The scattering peak shifts toward lower angles, lower values of s, with increasing molecular weight indicating that the long period increases. s is the magnitude of the scattering vector, **s**, and is given by

$$s = \frac{2 \sin \theta}{\lambda} \tag{2}$$

where 2θ is the scattering angle, and λ is the wavelength of X-ray source. L, L_c and L_a associated with the lamellar stacks were determined from the one-dimensional correlation function, $\gamma(z)$, evaluated from the scattered intensity $I(s)$ by the following equation [24]

$$\gamma(z) = \int_0^\infty I(s)s^2 \cos(2\pi sz)\, \mathrm{d}s \tag{3}$$

where z is the direction along which the electron density is measured. The one-dimensional correlation function was obtained directly by Fourier transformation of the Lorentz-corrected intensity. As the experimentally accessible range of s is finite, it is necessary to extend the intensity to both lower and higher s values. The lower s values were obtained by linearly extrapolating from the smallest measured s value to zero. Data at higher s values ($s > 0.12\ \mathrm{nm}^{-1}$) were fitted to Porod's law [25]. Porod's law describes two-phase systems with sharp boundaries, and gives the relationship between the scattering intensity $I(s)$ with s at the limit of large s as

$$\lim_{s\to\infty} (I(s)) = K_p s^{-4} + B \tag{4}$$

B, a residual background term, was subtracted from the experimental data and the fitted value of the Porod constant, K_p, was used to extend the scattering intensity beyond the data limit of $s = 0.12\ \mathrm{nm}^{-1}$ as $I(s) = K_p s^{-4}$.

Fig. 2 is a typical one-dimensional correlation function of a SAXS pattern from PHBV derived in this way. Based on the SAXS analysis of PHB and PHBV by Rule and Liggat [26], L, L_c, and L_a can be determined from the correlation function curve in Fig. 2. L_c is taken to be greater than L_a because of the high crystallinity of the material. Barham et al. [27] reported crystallinities between 60 and 80% for PHB and PHBVs from wide-angle X-ray measurements. Fig. 3 shows L, L_c and L_a as a function of the molecular weight of PHBV. It can be seen from Fig. 3 that all these three parameters increase as the molecular weight increases. The value of L increases from 7.73 to 8.31 nm, the value of L_c increases from 5.13 to 5.47 nm, and the value of L_a increases from 2.60 to 2.84 nm as the molecular weight increases from 53 000 to 262 000 g/mol.

Tanzawa et al. [28] studied the effect of molecular weight on the lamellar thickness of isotactic polystyrene crystallized at high supercoolings from dimethyl phthalate solution. They found that the lamellar thickness did not depend on supercooling (at high supercoolings) but increased with molecular weight. They explained this on the basis of loops existing in the molecular conformation in solution, finding by calculation that the length of such loops agreed with the limiting lamellar thickness and increased with the polymer molecular weight.

In a more comprehensive study of the melt crystallization of several polymers, Robellin-Souffache and Rault [16] found that long period increased with the square root of molecular weight. The increase in thickness was confined to the interlamellar region, while the crystal thickness remained constant and the crystallinity fell. The model for this was the trapping of molecular coils in interlamellar regions when distant parts of the same large molecule began to crystallize in adjacent lamellae. This behavior

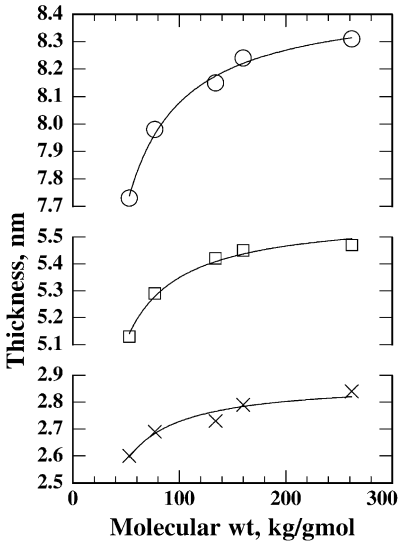

Fig. 3. Effect of molecular weight on the long period, lamellar and amorphous thicknesses for PHBVs. (○) Long period, (□) lamellar thickness, (×) amorphous layer thickness. The curves are of the form $A - B/M_w$.

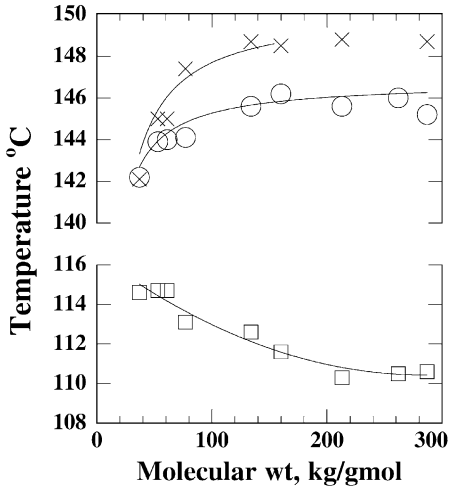

Fig. 4. Effect of molecular weight on the melting and non-isothermal crystallization temperatures for PHBVs. (○) T_m measured in the first run, (×) T_m measured in the second run, (□) T_c measured in the cooling run. The curves for the melting temperatures are of the form $A - B/M_w$.

was said to be completely general, and this was supported by a later study of PEEK [29]. However, all the polymers studied were homopolymers.

In the present study, where PHBV, a copolymer, was crystallized from the melt, the long period was found to increase with the molecular weight, which is in general agreement with the previous findings [16,28,29]. The long period, lamellar thickness, and amorphous layer thickness are similar to those reported by Rule and Liggat [26], who correlated the morphological parameters with annealing temperatures and HV contents. The lines that pass accurately through the data in Fig. 3 are of the form $A - B/M_w$. That is, the long period and the crystal thickness both vary linearly with the inverse of the molecular weight. This is not the functional dependence on molecular weight predicted for homopolymers [16] but since copolymerization has its own effect on crystal size and crystallinity it seems likely that this model would need modification.

3.2. Thermal analysis

Table 2 shows the glass transition temperature, T_g, the melting temperatures, T_m, and melting enthalpies, ΔH_m, for first and second heating scans, and the non-isothermal crystallization temperature, T_c, during the cooling scan, of all the PHBV specimens. The first heating run was to measure the crystalline structure, including the melting temperature and crystallinity, formed during the isothermal crystallization (annealing), while the second heating run was to measure the crystalline structure formed during the non-isothermal crystallization.

Fig. 4 shows the plots of melting temperature, T_m, for the first and second runs, and non-isothermal crystallization temperatures, T_c, during the cooling run as a function of molecular weight, $\bar{M}_w$, of PHBV. It can be seen from Fig. 4 and Table 2 that the melting temperature increases from 142 to 146 °C in the first run, and from 142 to 149 °C in the second run as the molecular weight increases from 37 000 to 287 000 g/mol. However, non-isothermal

Table 2
Effect of molecular weight on the thermal properties of PHBV

$\bar{M}_w$ (g/mol)	T_g (°C) (first scan)	T_m (°C)		ΔH_m (J/g)		T_c (°C)
		First scan	Second scan	First scan	Second scan	
37 000	−0.1	142.2	142.1	75.1	79.9	114.6
53 000	−0.7	143.9	145.0	72.3	79.5	114.7
61 000	1.8	144.0	145.0	69.2	77.5	114.7
77 000	1.5	144.1	147.4	68.7	77.2	113.1
134 000	0.7	145.6	148.7	68.7	76.3	112.6
160 000	2.0	146.2	148.5	67.3	76.1	111.6
213 000	1.9	145.6	148.8	66.8	74.3	110.3
262 000	1.9	146.0	149.2	65.4	73.1	110.5
287 000	1.5	145.2	148.7	61.9	73.2	110.6

crystallization temperature decreases from 115 to 110 °C in the cooling run for the same specimens. When molecular weight is above 130 000 g/mol, melting temperatures and non-isothermal crystallization temperatures seem to level off.

Since thicker crystals melt at higher temperatures, the results on melting temperatures in the first heating run are in general agreement with the lamellar structure derived from the SAXS analysis. The lines drawn through the melting temperatures in Fig. 4 are again of the form $A - B/M_w$. That is, the melting temperature varies linearly with the inverse of the molecular weight. Combining this with the results shown in Fig. 3 leads by simple algebra to the conclusion that the melting temperature is a linear function of long period or crystal thickness. Specifically, T_m (°C) = 113.3 + 3.9L (nm) or T_m (°C) = 111.0 + 6.43L_c (nm).

Clearly, these empirical equations have a limited range of applicability; they predict that a crystal of infinite thickness has an infinite melting point, and that a crystal of vanishing thickness melts at about 112 °C. Neither of these predictions can be correct. The conditions used here give a narrow range of long periods and of melting temperatures well away from T_m^0. Thus, the true relation between T_m and L may be more complex, although well approximated as linear over this narrow range.

The usual equation relating T_m to L_c is thermodynamic, from the energy balance in equilibrium melting, and is

$$T_m = T_m^0 - \frac{2\gamma T_m^0}{\Delta H_f L_c} \quad (5)$$

where T_m^0 is the melting point of an infinite crystal, γ is the fold surface free energy, and ΔH_f is the enthalpy of fusion. For a single material prepared at different long period, these parameters are often taken as constant giving a melting point depressed by an amount proportional to $1/L_c$, $T_m = T_m^0 - C/L_c$.

There is no real discrepancy between these expressions as the conditions that lead to them are very different—the same thermal history on a range of different molecular weights in one case, and the same material crystallized at different temperatures in the other. Different molecular weights may be expected to lead to different degrees of non-equilibrium behavior such as reorganization on melting, and to different values of the parameters in Eq. (5).

The difference in melting temperatures observed between the first and second heating runs is due to the difference in crystallization conditions. The first heating run melts material crystallized at 80 °C or below, while the material melted in the second run crystallized above 110 °C. The low molecular weight material, below 37 000 g/mol, is presumably able to reach perfection even at the lower growth temperature. As for the change in re-crystallization temperature, it is to be expected that the rates of crystallization drop at higher molecular weight, so the peak crystallization occurs at lower temperatures on cooling higher molecular weight material.

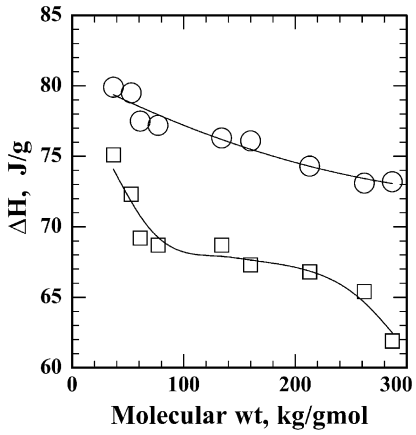

Fig. 5. Effect of molecular weight on the melting enthalpies for PHBVs. (□) ΔH_m measured in the first run, (○) ΔH_m measured in the second run.

Fig. 5 is a plot of melting enthalpy in the first and second heating runs as a function of molecular weight of PHBV. The lines drawn in Fig. 5 are simply aids to the eye. The melting enthalpy has an opposite trend to that of the melting temperature. In the first and second heating runs, the melting enthalpy decreases from 75.1 to 61.9 J/g, and from 79.9 to 73.2 J/g when the molecular weight increases from 37 000 to 287 000 g/mol, respectively. As no data on the equilibrium melting enthalpy, ΔH_m^0, are available for the material used in this study, PHBV with 9% HV content, crystallinities were not calculated from the measured enthalpies. However, ΔH_m^0 should be reasonably constant, and so the experimental enthalpy should be a measure of the crystallinity for all the PHBV samples. These results, therefore, indicate that crystallinity decreases as the molecular weight of PHBV increases. The crystallinities are different for the first and second heating runs. The higher crystallinity for the second melting is to be expected since the first crystallization took place at a lower temperature.

In general, the degree of crystallinity depends on several factors including the chemical structure, molecular weight, and thermal treatment. Here, the thermal history of the samples was exactly the same in each run, and the chemical structure is not affected by the thermal degradation that reduced the molecular weight [10–14,19]. Differences in crystallinity of different specimens were produced only by the molecular weight, that is, at different molecular weights the same thermal treatment was not equivalent in its effect. Fig. 5 shows that the effect of molecular weight was much greater in the material crystallized to a smaller extent at lower temperature.

It can be seen from Table 2 that molecular weight has little effect on T_g. There are two ways that molecular weight can influence the glass transition temperature. Chain ends are defects and the presence of more chain ends at lower molecular weight can add more free volume, reducing the constraints on the chains and reducing T_g. But as discussed earlier, PHBVs with lower molecular weight have higher

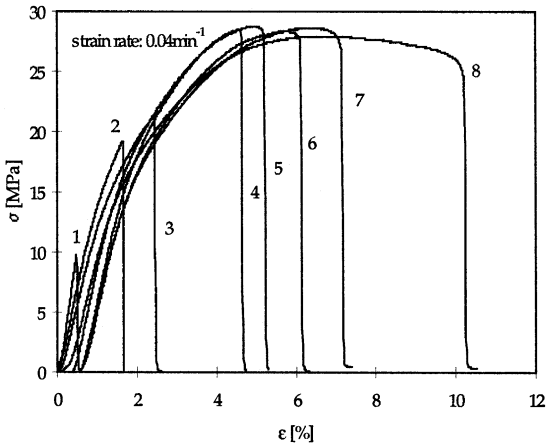

Fig. 6. Typical tensile stress versus strain plots for PHBVs with different molecular weights. (1) 37 000, (2) 53 000, (3) 61 000, (4) 77 000, (5) 134 000, (6) 160 000, (7) 213 000, (8) 262 000 g/mol. The starting points were shifted to have a better identification of the initial parts of the curves.

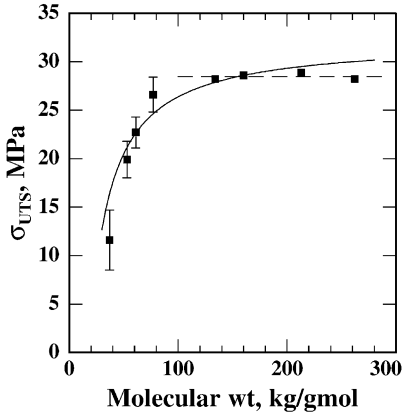

Fig. 7. Ultimate tensile strength versus molecular weight for PHBVs. The solid line through the data is a fit of Eq. (6) excluding the point at the highest molecular weight. Above 100 kg/g mol the errors are small, of the scale of the symbol size, and the dashed line shows that the strength is constant in this region.

crystallinity, and more crystals increase the constraints on the amorphous chains, raising T_g. It appears that in the case of PHBVs the effects largely cancel each other out, and there is no distinct variation of T_g with molecular weight for the thermal treatment used here.

3.3. Tensile properties

Fig. 6 presents typical stress versus strain plots for PHBVs with different molecular weights. Ultimate tensile strength, σ_{uts}, its corresponding strain, ε_{uts}, and Young's modulus, E, were calculated from the plots and averaged from at least five specimens. The data are summarized in Table 3. Fig. 7 is a plot of ultimate tensile strength versus molecular weight that illustrates a strong dependence of σ_{uts} on molecular weight. At very low molecular weight, PHBV was extremely brittle and no data could be obtained. This is the reason why no thermal or mechanical data is presented for molecular weights below 37 000 g/mol. σ_{uts} increases rapidly as the molecular weight increases and then levels off. Increasing the molecular weight from 37 000 to 134 000 g/mol causes an increase of σ_{uts} from 11.6 to 28.2 MPa. Further increase of molecular weight has essentially no effect on σ_{uts}. The reproducibility and thus the accuracy of the strength measurement are much greater above 100 000 g/mol.

It can be seen from Fig. 8 that Young's modulus varies from 1.5 to 1.3 GPa for PHBVs with different molecular weights. Young's modulus is often unaffected by morphological details, but should be affected by crystallinity. Crystallinity decreases by 16% as the molecular weight increases, while the modulus decreases by 13% and this looks like agreement. But compare the modulus in Fig. 8 to the lower curve in Fig. 5, which tracks the sample crystallinity and it is clear that there is no simple or direct relation between the two. The modulus falls more than the crystallinity at high molecular weight, and at low molecular weight is constant or increasing as crystallinity falls. Clearly other factors are coming into play, but it is not clear what these factors are.

Table 3
Effect of molecular weight on the tensile properties of PHBV

$\bar{M}_w$ (g/mol)	σ_{uts} (MPa)	E (GPa)	ε_{uts} (%)
37 000	11.6 (27.12)[a]	1.4 (3.6)	0.9 (32.4)
53 000	19.9 (9.4)	1.5 (2.2)	1.8 (15.7)
61 000	22.7 (7.2)	1.5 (1.7)	2.3 (10.9)
77 000	26.6 (6.6)	1.5 (2.1)	3.5 (17.8)
134 000	28.2 (1.2)	1.5 (1.7)	4.5 (4.6)
160 000	28.6 (1.1)	1.5 (2.4)	5.2 (4.9)
213 000	28.9 (1.5)	1.4 (3.4)	5.4 (2.0)
262 000	28.2 (0.8)	1.3 (2.1)	5.9 (4.8)

[a] Numbers in parentheses are percentage coefficient of variation.

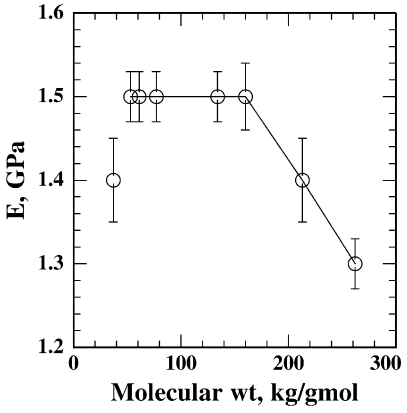

Fig. 8. Young's modulus versus molecular weight for PHBVs. There is a decline above 160 kg/g mol, but the change does not match the change in crystallinity (Fig. 5).

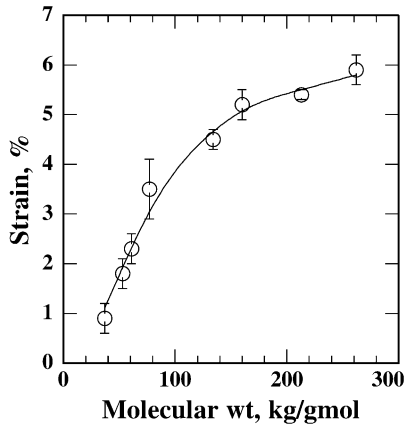

Fig. 9. The strain at the point of ultimate tensile strength versus molecular weight for PHBVs.

Fig. 9 is a plot of the strain at the point of ultimate tensile strength, ε_{uts}, versus molecular weight. As molecular weight increases from 37 000 to 77 000 g/mol, the strain increases from 0.9 to 3.5%. Further increase in molecular weight results in a continuous increase in ε_{uts}, but at a slower rate.

The relationship between ultimate tensile strength and molecular weight of a polymer is a very complicated issue, and theoretical understanding is difficult. An empirical equation has been used to describe this relationship [17,18] for a polymer with number average molecular weight M_n

$$\sigma_{uts} = A - \frac{B}{M_n} \tag{6}$$

where A and B are constants. This is derived from considering chain ends, with a concentration proportional to $1/M_n$, as defects reducing the strength. The line in Fig. 7 is a fit of Eq. (6) to the data, using our viscometry-derived M_w in place of M_n and excluding the point at the highest molecular weight. It can be seen that σ_{uts} and $\bar{M}_w$ follow Eq. (6) reasonably well, at least up to a molecular weight of 250 000. Alternatively, the data can be interpreted as a rapid rise in strength with molecular weight as the entanglement network becomes established and the failure mode changes from brittle to ductile. At higher molecular weights, the strength becomes constant as the higher ductility shown in Fig. 9 is balanced by the lower modulus shown in Fig. 8. The dashed line in Fig. 7 shows this constant strength value of 28.5 ± 0.4 MPa.

4. Conclusions

Molecular weight has a significant effect on the lamellar size and the thermal and mechanical properties of PHBV. For the thermal treatment used in this study, quenching and annealing, and for molecular weights above 37 000 g/mol, we conclude the following:

1. The lamellar thickness, the amorphous layer thickness, the melting temperature and the ultimate tensile strength of the sample all increase with an increase in molecular weight. All of these variables can be fitted by an empirical equation of the form $A - B/M_w$.
2. The crystallinity, as indicated by the melting enthalpy, and the non-isothermal crystallization temperature decrease with an increase in molecular weight.
3. Young's modulus generally falls as molecular weight increases, but this cannot be simply explained by the change in crystallinity. The strain at the point of ultimate tensile strength increases with an increase in molecular weight. As the molecular weight increases, the rate of increase of this failure strain slows down.

Acknowledgements

The College of Human Ecology of Cornell University provided the financial support for this work. We gratefully acknowledge the use of DSC of the Cornell Center for Materials Research (CCMR) supported through NSF Award DMR-0079992. This work is based in part upon research conducted at the Cornell High Energy Synchrotron Source (CHESS) which is supported by the National Science Foundation and the National Institutes of Health/ National Institute of General Medical Sciences under award DMR 9713424.

References

[1] Doi Y. Microbial polyesters. New York: VCH, 1990.
[2] Anderson J, Dawes EA. Microbiol Rev 1990;54:450.
[3] DeKoning GJM, Lemstra PJ. Polymer 1993;34:4089.
[4] DeKoning GJM. ACS Symp 1994;575:188.
[5] Steinbuchel A, Valentin HF. FEBS Microbiol Lett 1995;128:219.
[6] Barham PH, Keller A. J Polym Sci, Polym Phys Ed 1986;24:69.
[7] Barham PH. J Mater Sci 1984;19:392.
[8] Luo S, Netravali AN. Polym Compos 1999;20:367.
[9] Luo S, Netravali AN. J Mater Sci 1999;34:3709.
[10] Morikawa H, Marchessault RH. Can J Chem 1981;59:2306.
[11] Kunioka M, Doi Y. Macromolecules 1990;23:1933.
[12] Grassie N, Murray EJ, Holmes PA. Polym Degrad Stab 1984;6:47.
[13] Grassie N, Murray EJ, Holmes PA. Polym Degrad Stab 1984;6:95.
[14] Grassie N, Murray EJ, Holmes PA. Polym Degrad Stab 1984;6:127.
[15] Billingham NC, Henman TJ, Homes PA. In: Grassie N, editor. Developments in polymer degradation-7. London: Applied Science Publishers, 1987. Chapter 3.
[16] Robellin-Souffache E, Rault J. Macromolecules 1989;22:3581.
[17] Flory PJ. J Am Chem Soc 1945;67:2048.
[18] Ogawa T. J Appl Polym Sci 1992;44:1869.
[19] Luo S. PhD Dissertation. Cornell University; 2000.
[20] Akita S, Einaga Y, Miyaki Y, Fujita H. Macromolecules 1976;9:774.
[21] Grubb DT, Keller A. J Polym Sci, Phys Ed 1980;18:207.
[22] Voigt-Martin IG, Mandelkern L. J Polym Sci, Phys Ed 1984;22:1901.

[23] Strobl GR. The physics of polymers, concepts for understanding their structures and behavior. 2nd ed. Berlin: Springer, 1997.
[24] Strobl GR, Schneider M. J Polym Sci, Phys Ed 1980;18:1343.
[25] Glatter O, Krathy O, editors. Small angle X-ray scattering. London: Academic Press, 1983.
[26] Rule RJ, Liggat JJ. Polymer 1995;36:3831.
[27] Barker PA, Barham PH, Martinez-Salazar J. Polymer 1997;38:913.
[28] Tanzawa Y, Miyaji H, Miyamoto Y, Kiho H. Polymer 1988;29:904.
[29] Fougnies C, Dosiere M, Koch MHJ, Roovers J. Macromolecules 1998;31:6266.